Research Article Vol. 34, No. 4 / 23 Feb 2026 / Optics Express 6486
Optics EXPRESS

# High frequency-reproducibility nanosecond pulsed laser with high output power

JIE YANG,[1] YANLIN ZHANG,[2] WEIJIE LI,[1] XIAOJUN JIA,[1,3] HUADONG LU,[1,3,*] AND KUNCHI PENG[1,3]

[1]State Key Laboratory of Quantum Optics Technologies and Devices, Institute of Opto-Electronics, Shanxi University, Taiyuan 030006, China
[2]Institute of Molecular Science, Shanxi University, Taiyuan 030006, China
[3]Collaborative Innovation Center of Extreme Optics, Shanxi University, Taiyuan 030006, China
*luhuadong@sxu.edu.cn

**Abstract:** This paper reported a high frequency-reproducibility high-power single-longitudinal-mode (SLM) pulsed laser which was achieved by combining an etalon set, a pre-lasing process and a nonlinear optical frequency conversion (NOFC). The NOFC was used to rapidly enlarge the loss difference between the dominant mode and sub-modes. Then, the pre-lasing process was introduced before the pulse build-up to enhance the dominant-mode intensity. On this basis, an etalon set was inserted into the resonator to select a reference frequency. As a result, the frequency reproducibility between pulses was significantly improved. In the experiment, a type-I phase-matched LBO was used to introduce the NOFC. When the pre-lasing process was introduced by slightly lowering the loss induced by the Q-switch, the spectral width of the 1064 nm laser was narrowed from 32.80 pm to 14.40 pm, and the wavelength drift was improved from less than 1.20 pm to less than 0.36 pm. On this basis, the spectral width was further narrowed to 2.20 pm by improving the frequency reproducibility between pulses through employing an etalon set with thicknesses of 0.5 mm, 1 mm and 10 mm, and the wavelength drift was less than 0.07 pm.

© 2026 Optica Publishing Group under the terms of the Optica Open Access Publishing Agreement

## 1. Introduction

High-power pulsed lasers with the narrow spectral width are the preferred sources for many fields including high-resolution spectroscopy, coherent lidar and so on since their single-longitudinal-mode (SLM) characteristics and excellent frequency stability are essential to improve the signal-to-noise ratio and measurement precision of the detection system [1–4]. However, the pulse build-up time of a Q-switched nanosecond (ns) laser is so short that the round-trip number in the resonator is limited, which makes it difficult to realize SLM operation only through the mode competition. To address this issue, the simplest method is to insert mode-selection components into the cavity to increase the net-gain difference between the dominant mode and sub-modes. In 2011, Tong et al. realized a SLM pulsed 1064 nm laser with a repetition rate of 400 Hz and a pulse width of 6 ns by inserting an etalon into a twisted-mode cavity [5]. However, its average output power was only 0.5 W due to the large loss of the inserted etalon. In 2023, Song et al. employed a volume bragg grating (VBG) to realize a dual-wavelength SLM pulsed laser with a repetition rate of 1 kHz [6]. The pulse energy of 1064 nm and 532 nm was 0.55 mJ and 0.29 mJ, respectively, corresponding to a conversion efficiency of only 15% and 8%. However, it could be seen that the output power was severely restricted because of the large loss of the mode-selecting elements. On the contrary, the seed-laser-injection method is proposed and is becoming increasingly popular because of its intrinsic low loss. In 2015, Zhang et al. reported a seed-laser-injection single-frequency, ns pulsed Nd:YAG laser with a pulse energy of 9.9 mJ at a repetition rate of 400 Hz [7]. A $RbTiOPO_4$ (RTP) crystal was adopted to modify the optical path length of the slave laser based on the delay-ramp-fire technique, so that the slave laser could

#590156 https://doi.org/10.1364/OE.590156
Journal © 2026 Received 13 Jan 2026; revised 4 Feb 2026; accepted 6 Feb 2026; published 12 Feb 2026

Optics EXPRESS

be in resonance with the seed laser. However, this method exhibited a significant instability in frequency and output power (with a frequency jitter of 1.5 MHz over 2 min, and a power fluctuation of 0.3% over 23 min). In 2019, Cao et al. reported an optimized ramp-triggered seed-laser-injection method by employing a high-speed RTP electro-optic modulator (EOM) together with a fast linear scanning [8]. A stable single-frequency laser was realized in a zigzag slab Nd:YAG ring oscillator at a repetition rate of 20 Hz, a pulse energy of 67 mJ, and a pulse width of 19 ns. The frequency stability was 2.0 MHz over 7 min, and the timing stability was below 4 $\mu$s. In 2023, Yu et al. reported a nonplanar ring oscillator (NPRO) single-frequency seed-laser-injection scheme and combined a "ramp-hold-trigger" protocol with dual piezoelectric (PZT) feedback compensation to realize single-frequency 1319 nm pulsed laser output with a repetition rate of 500 Hz, a single-pulse energy of 2.3 mJ, and an average power of 1.15 W [9]. Based on this method, the pulse timing jitter was further reduced to below 3 ns. However, the seed-laser-injection method requires an additional laser as the seed laser and usually needs a locking system, resulting in the complex system. To reduce the complexity of the laser, a SLM pulsed laser can also be achieved by generating the seed laser inside the oscillator, such as with pre-lasing technology. In 2014, Lian et al. realized a SLM pulsed laser based on pre-lasing technology in an end-pumped acousto-optic (AO) Q-switched Nd:YAG ring-cavity with a repetition rate of 2 kHz, a pulse width of 475 ns and a peak power of 1.1 kW [10]. In 2020, Jin et al. reported a SLM Q-switched Pr:YLF laser by the pre-lasing technique combined with a Fabry-Perot etalon [2]. Under an absorbed pump power of 2.3 W and a repetition rate of 10 kHz, a maximum pulse energy of 3.94 $\mu$J and a pulse width of 81.1 ns were achieved, corresponding to a peak power of only 48.5 W. Compared to other methods, the AO Q-switched lasers with pre-lasing have the advantages of a simple system, the ability to easily achieve high repetition rate, and controllable synchronization with an external signal [11,12]. However, solely depending on the pre-lasing technology to achieve a SLM pulsed laser would consume so many inversion particles during the pre-lasing period that the output power was restricted and the pulse width was expanded. In 2025, our group reported what we believe to be a novel method to achieve high-power SLM pulsed lasers with the assistance of the nonlinear optical frequency conversion (NOFC) [13]. On this basis, in this paper, we propose a method to improve the frequency reproducibility of a ns pulsed laser, which is implemented by combining the pre-lasing, mode-selecting with the NOFC processes. A preferred longitudinal mode is selected out by the employed etalon set and acts as the reference frequency during the pulse build-up process. To ensure that the selected preferred longitudinal mode has absolute priority over other modes, a pre-lasing process is introduced before the pulse buildup to extend the mode-selection time of the etalon. After the loss introduced by the Q-switch is removed, the selected longitudinal mode is rapidly amplified. The introduction of the NOFC ensures that the sub-modes are rapidly annihilated within a short time [14,15]. As a result, a stable SLM 1064 nm pulsed laser was obtained with a repetition rate of 4 kHz, a spectral width of 2.20 pm, and an average output power of 4 W.

## 2. Fundamental principles

In order to analyze the influence of the method we proposed above on the mode-selection in pulsed lasers in detail, the dynamics presented above are simulated using the rate equations. For a ring laser resonator, the multi-mode rate equations are given by [16]:

$$\begin{cases} \frac{dn}{dt} = -\gamma c \sum_j \phi(\nu_j)\sigma(\nu_j)n - \frac{n}{\tau_c} + P \\ \frac{d\phi(\nu_j)}{dt} = \frac{\phi(\nu_j)}{t_r}\left\{\sigma(\nu_j)nl - [\ln(\frac{1}{R}) + \delta]\right\} + S \end{cases} \tag{1}$$

where $\phi$ is the intracavity photon number density, $n$ is the density of inverted particles in the gain medium, $\gamma$ can be thought of as an "inversion reduction factor" since it corresponds to

Optics EXPRESS

the net reduction in the population inversion after the emission of a single photon, $\sigma$ and $l$ are the stimulated-emission cross section and the length of the gain medium, respectively, $R$ is the reflectivity of the output-coupling mirror, $\delta$ is the one-way intracavity photon loss factor including diffraction, scattering, absorption, etc., $t_r$ is the round-trip time for intracavity photons, $c$ is the speed of light in vacuum, and $\tau_c$ is the lifetime of the inverted population in the gain medium, $\nu_j$ is the optical frequency of the j-th longitudinal mode, $P$ is the average pump rate, $\tau_c = l_c/[c(L - \ln R)]$, and $l_c$ is the effective optical length of the resonator. The parameter $S$ denotes the fraction of spontaneous-emission photons coupled into the lasing mode and represents the contribution of spontaneous-emission to stimulated emission.

When nonlinear loss is introduced into the resonant cavity, the loss factor $\delta$ becomes [17]:

$$\delta' = \delta + l_{NL} \tag{2}$$

$$l_{NL}(\nu_j) = kI(\nu_j) + 2k \sum_{i \neq j} I(\nu_j) \tag{3}$$

By substituting Eq. (2) and (3) into Eq. (1) and numerically solving it using the fourth-order Runge-Kutta method, the dynamic of the resonator can be obtained.

Figure 1 illustrates the dynamics of an active Q-switched laser before and after introducing the pre-lasing process, where $l_Q$, $n$, and $\phi$ are the loss induced by the Q-switch, the inverted population density and the photon density, respectively. In order to analyze the intensity evolution of different longitudinal modes detailly, three adjacent longitudinal modes labeled as the -1 mode, 0 mode, and +1 mode successively centered on the wavelength of 1064 nm are calculated. The entire dynamic process is divided into two periods, including the energy storage period and pulse build-up period, as shown in Fig. 1($a_1$). In the energy storage period, $l_Q$ is at its maximum value of 100% to realize the population inversion, as shown in Fig. 1($a_2$). When the population inversion is completed, once the loss induced by the Q-switch is completely removed, a SLM pulse is generated, as shown in Fig. 1($a_{31}$). Although the NOFC process can realize a pulsed SLM laser, two additional longitudinal modes still exist at the rising edge of the pulse waveform because it is very difficult to completely suppress the oscillation of the sub-modes within a short period of time only depending on the mode competition. However, when a pre-lasing process is introduced before the pulse build-up, the dominant longitudinal mode has enough time to form an absolute priority over other modes. As a result, the sub-modes can easily be suppressed completely. Figure 1($b$) shows the pre-lasing mechanism by manipulating the loss induced by Q-switch $l_Q$. The energy storage period in Fig. 1($a$) is divided into two periods, including the energy storage period and pre-lasing period, as shown in Fig. 1($b_1$). Different from the dynamics in Fig. 1($a_1$), when the population inversion is completed during the energy storage period, the cavity loss is then reduced to the laser threshold by slightly lowering the value of $l_Q$, thus the pre-lasing process is introduced. During this long pre-lasing period, the preference of dominant longitudinal mode is significantly enhanced, as shown in Fig. 1($b_{31}$). On this basis, once the loss induced by the Q-switch is completely removed, a SLM pulse is generated without other two longitudinal modes presented even at the beginning of the pulse build-up, as shown in Fig. 1($b_{32}$).

Although a pulsed SLM laser is free of sub-longitudinal-modes existing at the rising edge of the pulse by combining the NOFC with the pre-lasing process, the frequency difference between pulses will easily observe because the dominant longitudinal-mode between pulse drifts between several longitudinal-modes. Specifically, for most lasers, the oscillating priority of the different longitudinal modes in the resonator is mainly determined by the gains of the laser crystals. However, the gain values of several longitudinal modes near the center of the gain curve are almost equal. Therefore, under the high-power pump, any of them may become the dominant mode due to the environmental disturbances, thermal instability, mechanical instability and so on. To address this issue, it is necessary to introduce a frequency reference to improve the frequency reproducibility. For this purpose, an etalon set is inserted into the resonator to select a preferred

Optics EXPRESS

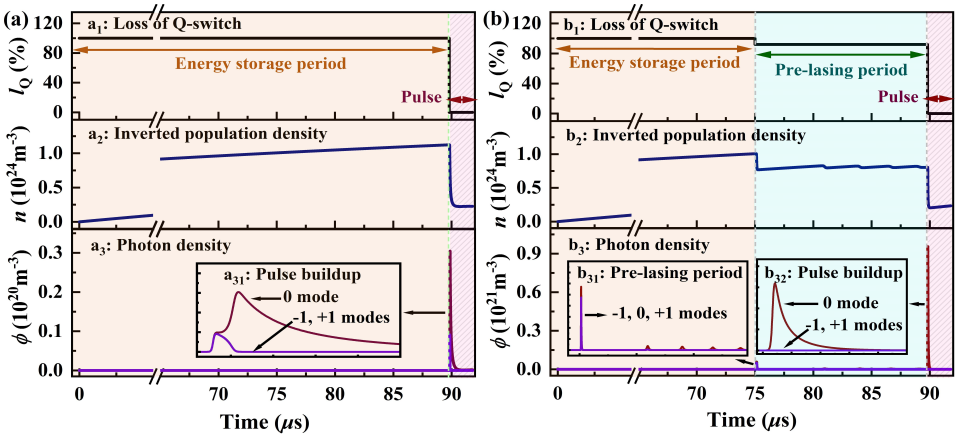



**Fig. 1.** The dynamics of an active Q-switched laser before (a) and after (b) introducing the pre-lasing process.

longitudinal-mode at the beginning of pulse build-up, as shown in Fig. 2. In Fig. 2(a) to (c), the center of the gain curve is successively moved to the three adjacent longitudinal modes previously specified to characterize the red or blue shift phenomenon of the fluorescence peak caused by thermal instability. When the etalon set is not inserted into the cavity, the final oscillating longitudinal-mode corresponds to the center wavelength of the gain profile. Nevertheless, when a quartz etalon set with thicknesses of 0.5 mm, 1 mm and 10 mm is inserted into the cavity, its transmission curve is shown in Fig. 2(d) where the reflectivity of each etalon is 5%, the final existing longitudinal mode is determined by the transmission peak of the etalons. Hence, the etalon can effectively improve the frequency reproducibility among different pulses in the pulsed laser.

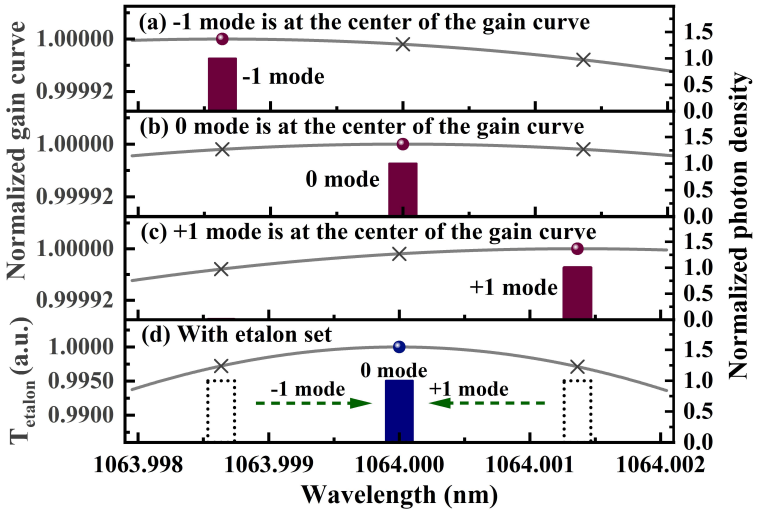



**Fig. 2.** The longitudinal modes distribution when the center of gain profile is successively moved to the three adjacent longitudinal mode without etalon set (a-c) and with etalon set (d).

Optics EXPRESS

## 3. Experimental setup

In order to verify the feasibility of the method we proposed above, the experimental setup was built and shown in Fig. 3. An a-cut, single-end-bonded composite $YVO_4$/Nd:$YVO_4$ crystal acted as the gain medium and was directly end-pumped by a laser diode (LD) with a center wavelength of 888 nm and a peak power of 200 W. The LD was operated in a pulsed mode with a repetition rate of 4 kHz and a pump duration of 75 $\mu$s. The pump beam was output from a fiber with a numerical aperture of 0.22 and was focused into the gain crystal Nd:$YVO_4$ using a telescope coupling system composed of two plano-convex lenses with focal lengths $f_1$ = 30 mm and $f_2$ = 100 mm. The Nd:$YVO_4$ crystal dimensions were $3 \times 3 \times (3 + 17)$ mm$^3$, comprising a 17-mm-long doped segment (0.8 at.%) and a 3-mm-long undoped segment. The resonator was configured as a four-mirror bow-tie ring cavity. $M_1$ and $M_2$ were both plano-convex mirrors with a curvature radius of 1500 mm. The plano-surface was coated with the antireflection (AR) film at 888 nm, and the convex surface was coated with AR films at 888 nm and highreflection (HR) films at 1064 nm. $M_3$ was a flat mirror coated with the HR film at 1064 nm. $M_4$ served as the output coupler with a transmission of 50% at 1064 nm and high transmission (HT) at 532 nm. To ensure the unidirectional operation, an optical directional (OD) device composed of a 45° rotator and a $\lambda/2$ waveplate was inserted into the cavity. The etalon set (the reflectivity of each etalon is 5%) was inserted into the cavity to select a reference frequency. A stable AO Q-switch (QS041-10G-IN2, GOOCH & HOUSEGO) was employed to accomplish the pulse generation, and the cavity loss was modulated by controlling the radio frequency (RF) power of the driver (CARD-FD2-041-24D24C-1AH-AF, CASTECH). A type-I noncritical phase-matched LBO crystal ($\theta$ = 90°, $\phi$ = 0°) with a size of $3 \times 3 \times 18$ mm$^3$ was inserted to introduce NOFC.

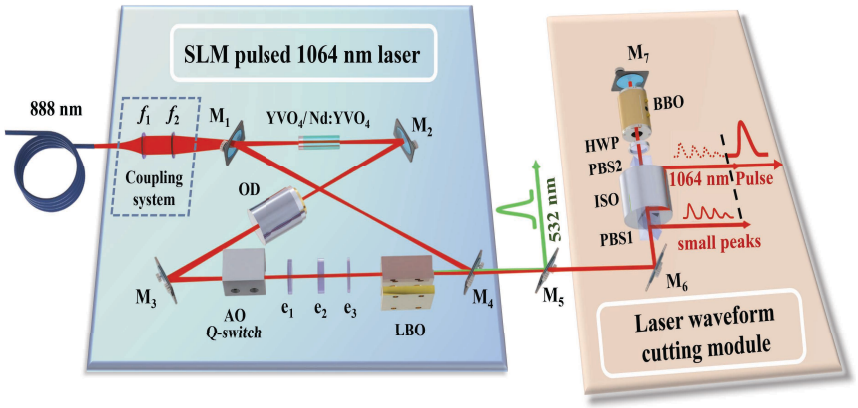



**Fig. 3.** Experimental setup for an all-solid-state SLM pulsed 1064 nm laser based on the combined etalon and NOFC.

Due to the introduction of the pre-lasing, there will be several small peaks arising from the damping oscillation of inverted population and laser intensity near the laser threshold [10]. To separate the small peaks, a laser waveform cutting module was designed by rapidly changing the laser polarization with EOM. Specifically, this module consists of an optical isolator (ISO), a BBO EOM, and a plane mirror with HR film at 1064 nm. When a quarter-wave voltage was applied to the EOM and the laser passes through it twice, the polarization of the laser was changed from horizontal polarized state to vertical polarized state and eventually reflected by PBS2 which was attached to the ISO. On the contrary, when no voltage was applied to EOM, the laser was reflected by PBS1. In this experiment, the voltage was applied to EOM only when the pulse passed through it. Therefore, these small peaks were reflected in PBS1 and the pulse was reflected in PBS2.

Optics EXPRESS

## 4. Results and discussion

In the experiment, the diffraction efficiency of AO Q-switch was changed by adjusting the radio frequency power controlled by an analog signal (5 V corresponds to the highest diffraction efficiency, while 0 V corresponds to 0), enabling real-time manipulation of the cavity loss to meet the requirement for pre-lasing. The diagram of analog signal voltage setting was shown in Fig. 4(a). The voltage of the AB segment was designed to be 5 V to achieve population inversion. The voltage of the CD segment was adjusted to slightly lower cavity loss, thus introducing the pre-lasing process. The voltage of the CD segment was set to be 0 V to remove the diffraction of AO Q-switch, thus forming a laser pulse. In addition, the temperature of LBO was controlled at 149° with a precision of 0.01° to maintain the optimum conversion efficiency of NOFC throughout the experiment.

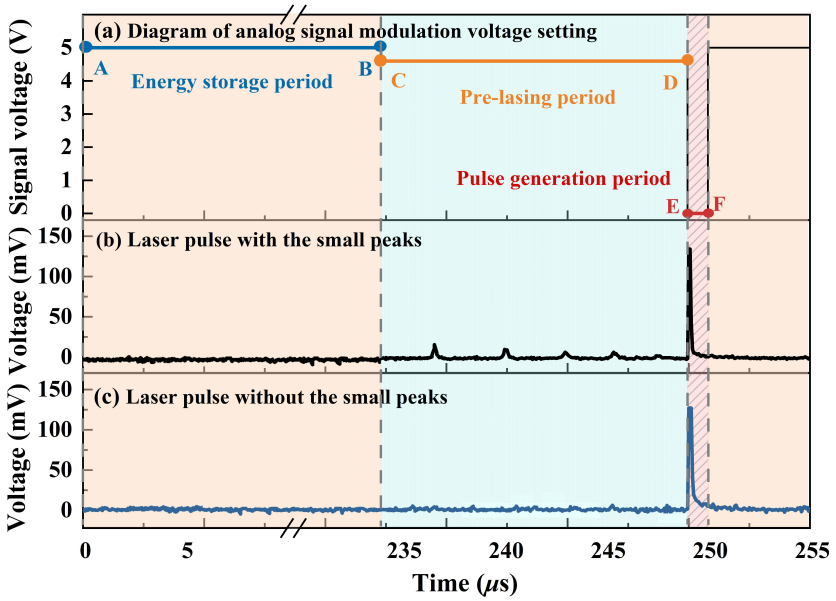



**Fig. 4.** (a) Diagram of analog signal modulation voltage setting. (b) Laser pulse with the small peaks. (c) Without the small peaks.

In our experiment, the values of segment durations (AB, CD, and EF) were obtained by reading the signal output from the signal generator. When the duration of the AB segment was designed to be 234 $\mu$s, the voltage of the CD segment was set to 4.6 V with a duration of 14.8 $\mu$s, and the duration of the EF segment was set to be 980 ns, the pre-lasing process was introduced, as shown in Fig. 4(b). The duration of each segment in the figure was measured by the oscilloscope cursor, and there is a deviation of about 0.09% between the sum and the theoretical period. This difference is within the typical uncertainty range of the oscilloscope sampling rate and cursor interpretation used. From Fig. 4(b), it can be seen that a series of small peaks emerged before the main pulse. The small peaks were separated from the main pulse by utilizing the laser waveform cutting module described in the experimental setup, as shown in Fig. 4(c). In this case, the average output power was reduced from 7.6 W to 5.9 W under the average pump power of 45 W.

Figure 5 shows the result after the pre-lasing process was introduced. The spectral width measured with a high-precision spectrometer (LSA 2R, HighFinesse) was narrowed from 32.80 pm to 14.40 pm. Furthermore, to obtain a SLM pulsed laser with high frequency reproducibility and narrow spectral width, the frequencies of all pulses of the 1064 nm laser were stabilized to the transmission peak of the etalon set.

Optics EXPRESS

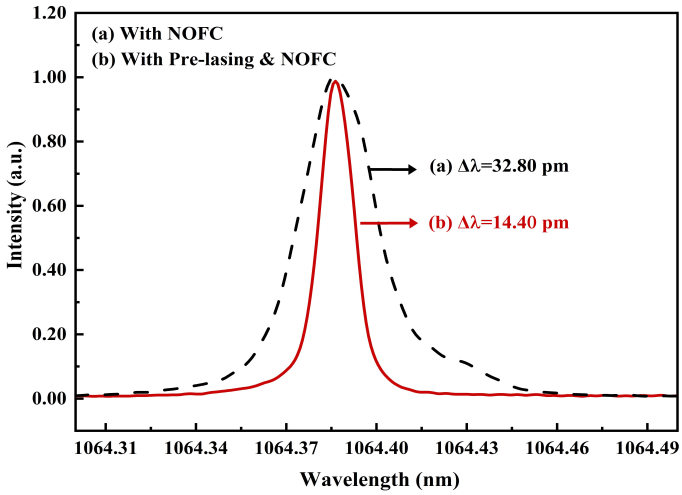



**Fig. 5.** Spectral width without (a) and with (b) the pre-lasing process.

In the experiment, the etalons with thicknesses of 0.5 mm, 10 mm, and 1 mm were inserted into the cavity successively to enhance the priority of the longitudinal mode selected by the etalon set. Since the reflectivity of each etalon is only 5%, the transmission bandwidth of the etalon set is so broad (see Fig. 2) that the locking between the etalon and the longitudinal mode of cavity was not necessary. What's more, as the etalon set is only used to provide reference frequency determined by its transmission peak, the loss induced by the etalon set is significantly reduced for the very low reflectivity. Those two advantages are essential differences from the traditional mode-selection method based on the etalon. The spectral width was narrowed from 14.40 pm to 10.80 pm when only the 0.5 mm etalon was employed. With the successive insertion of 10 mm etalon and 1 mm etalon, the spectral width was further narrowed to 6.80 pm and 2.20 pm, as shown in Fig. 6.

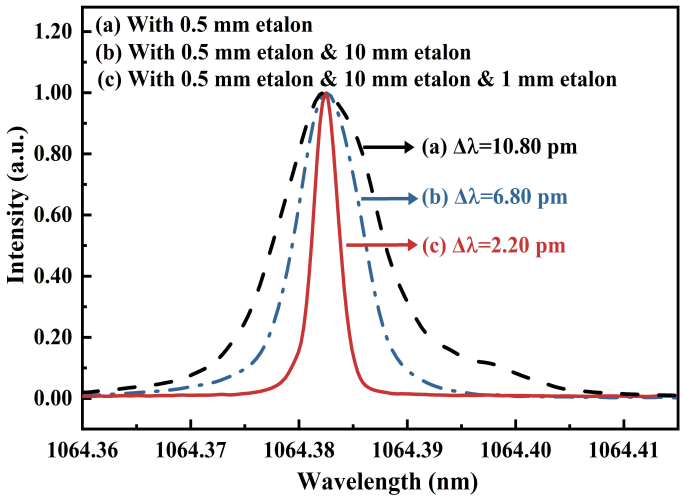



**Fig. 6.** Narrowed spectrum after inserting the etalon set.

Optics EXPRESS

Figure 7 shows the evolutions of spectral width stability and wavelength drift after the pre-lasing process and the etalon set were successively introduced into the resonator. In the case of SLM operation achieved through NOFC in a Q-switched laser, the spectral width stability was 2.42% and the wavelength drift was less than 1.20 pm within 30 minutes. In this case, when the pre-lasing process was introduced, the stability was further improved to 1.86%, and the wavelength drift was less than 0.36 pm. On this basis, when the etalon set was inserted into the resonator, the stability was significantly improved to 1.14%, and the wavelength drift was less than 0.07 pm.

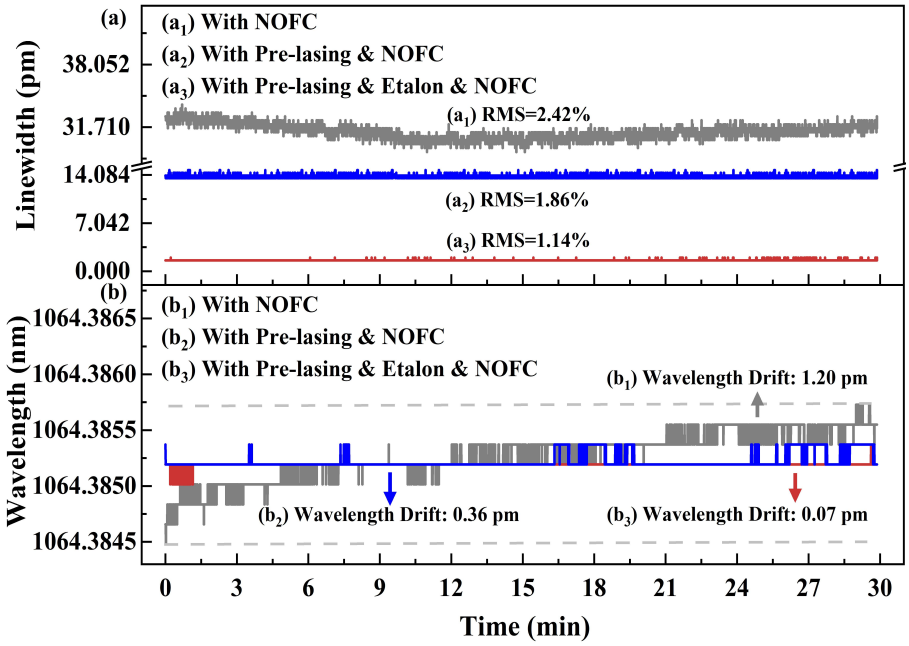



**Fig. 7.** Comparison of spectral width before and after narrowing of 1064 nm pulsed laser. (a) Relative stability of spectral width. (b) Wavelength drift.

Based on the above method for narrowing the spectral width, a frequency-stabilized narrow spectral width 1064 nm pulsed laser with a repetition frequency of 4 kHz and an average output power of 4 W was experimentally achieved. The output power curve at 1064 nm was measured with the assistance of a power meter (PM300-50, Coherent). The results were shown in Fig. 8(a). The pulse width of the 1064 nm laser measured by a high-speed photodetector is 24.29 ns (DET10A2, Thorlabs), as shown in Fig. 8(b), corresponding to a peak power of 43.23 kW and a single pulse energy of 1.05 mJ. The spectral width of the 1064 nm laser is 2.20 pm, as shown in Fig. 8(c). The beam quality factors $M_x^2$ = 1.01 and $M_y^2$ = 1.02 were measured using a beam quality analyzer (BC207VIS/M, Thorlabs), as shown in Fig. 8(d).

## 5. Conclusions

This paper reported a high frequency-reproducibility high-power SLM pulsed laser, which was achieved by combining an etalon set, a pre-lasing process and a NOFC. The NOFC was used to rapidly enlarge the loss difference between the dominant mode and sub-modes. Then, the pre-lasing process was introduced before the pulse build-up to enhance the dominant-mode intensity. On this basis, an etalon set was inserted into the resonator to select a reference frequency. In this case, the frequency reproducibility between pulses was significantly improved. In the experiment, a type-I phase-matched LBO crystal was used to introduce the NOFC. When the pre-lasing process was introduced by adjusting the analog signal voltage of the Q-switch from 5

Optics EXPRESS

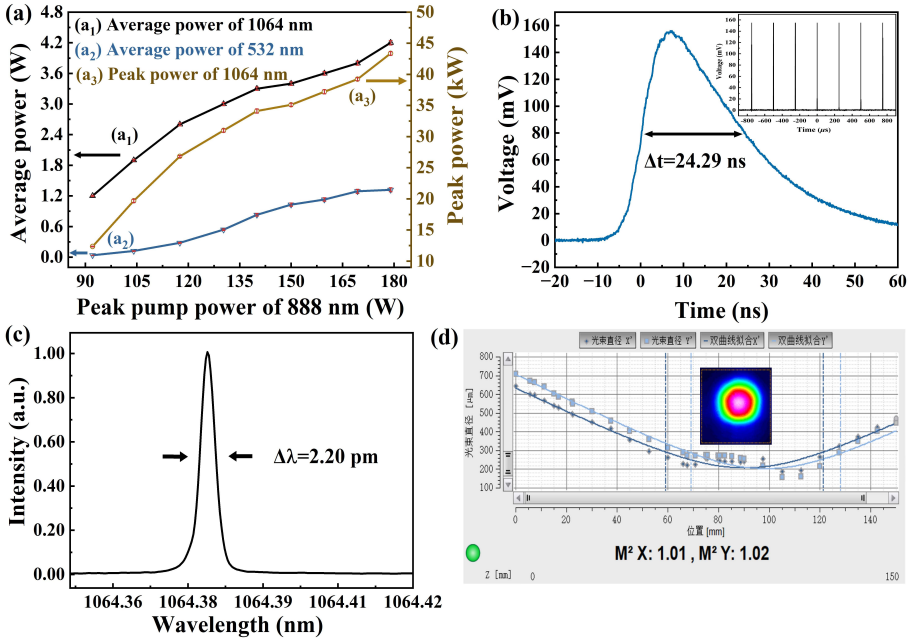



**Fig. 8.** Measured parameters of the 1064 nm pulsed laser. (a) Output power varies with pump power. (b) Pulse waveform and pulse sequence. (c) Spectral width. (d) Beam quality of $M^2$.

V to 4.6 V, the spectral width of the 1064 nm laser was narrowed from 32.80 pm to 14.40 pm, and the wavelength drift was improved from less than 1.20 pm to less than 0.36 pm. On this basis, the spectral width was further narrowed to 2.20 pm by improving the frequency reproducibility between pulses through an etalon set including a 0.5 mm etalon, 1 mm etalon and 10 mm etalon, and the wavelength drift was less than 0.07 pm. The achieved average output power of 1064 nm laser is 4 W with a repetition rate of 4 kHz and a pulse width of 24.29 ns, corresponding to a peak power of 43.23 kW and a single pulse energy of 1.05 mJ. Compared with traditional methods for realizing SLM pulsed lasers, this spectrum-narrowed SLM pulsed laser has the advantages of simple structure and high reliability, and it has important applications in lidar, plasma physics, and so on.

**Funding.** National Natural Science Foundation of China (62575163); National Key Research and Development Program of China (2022YFC2204003); The First Lab - National Innovation Center (Shanxi) science and technology innovation project; Funding from the National Key Laboratory of Particle Transport and Separation Technology (KWKF-2024-2).

**Disclosures.** The authors declare no conflict of interest.

**Data availability.** Data underlying the results presented in this paper are not publicly available at this time but may be obtained from the authors upon reasonable request.

## References

1. S. Luo, Z. Cai, H. Xu, *et al.*, "Direct oscillation at 640-nm in single longitudinal mode with a diode-pumped Pr:YLF solid-state laser," Opt. Laser Technol. **116**, 112–116 (2019).
2. L. Jin, W. Dai, Y. Yu, *et al.*, "Single longitudinal mode Q-switched operation of Pr:YLF laser with pre-lase and Fabry-Perot etalon technology," Opt. Laser Technol. **129**, 106294 (2020).
3. B.-Q. Yao, X.-M. Duan, D. Fang, *et al.*, "7.3 W of single-frequency output power at 2.09 $\mu$m from an Ho:YAG monolithic nonplanar ring laser," Opt. Lett. **33**(18), 2161–2163 (2008).
4. H. Zhang, M. Long, H. Deng, *et al.*, "Space debris laser ranging with a 60 W single-frequency slab nanosecond green laser at 200 Hz," Chin. Opt. Lett. **17**(5), 051404 (2019).

Optics EXPRESS


5. L. Tong, Z. Zhao, L. Cui, *et al.*, "400-Hz pulsed single-longitudinal-mode Nd:YAG laser with more than 100-mJ pulse energy and good beam quality," Laser Phys. **21**(1), 52–56 (2011).
6. Z. Song, Y. Li, Z. Yu, *et al.*, "Dual-wavelength single-longitudinal-mode sub-ns lasers with high pulse repetition frequency," Laser Phys. Lett. **20**(1), 015001 (2022).
7. J. Zhang, X. Zhu, X. Ma, *et al.*, "Stable seeder-injected Nd:YAG pulsed laser using a $RbTiOPO_4$ phase modulator," Chin. Opt. Lett. **13**(11), 111404–111408 (2015).
8. X. Cao, F. Lu, X. Wang, *et al.*, "Frequency stabilization of an injection seeded Nd:YAG ring oscillator by ramp-fire technique with a $RbTiOPO_4$ modulator," Appl. Phys. B **125**(9), 164 (2019).
9. G. Yu, C. Fang, J. Ding, *et al.*, "1319 nm single-frequency injection seeded Q-switched laser based on ramp-hold-fire," Proc. SPIE **12959**, 129590T (2023).
10. T. Lian, S. Wang, D. Cai, *et al.*, "High repetition rate, high peak power, pulsed single-longitudinal-mode Nd:YAG laser by self-injection-seeding," Opt. Commun. **323**(15), 154–161 (2014).
11. C. Bollig, W. A. Clarkson, and D. C. Hanna, "Stable high-repetition-rate single-frequency Q-switched operation by feedback suppression of relaxation oscillation," Opt. Lett. **20**(12), 1383–1385 (1995).
12. P. Yan, M. Gong, T. Xie, *et al.*, "Stabilization of pulse-to-pulse energy and width by gain-controlled prelase in laser-diode-pumped Q-switched laser," Opt. Eng. **42**(1), 159–162 (2003).
13. Y. Zhang, P. Jin, J. Yang, *et al.*, "Spectral purity improvement of high-power pulsed lasers achieved by manipulating the nonlinear optical frequency conversion," Opt. Lett. **50**(10), 3341–3344 (2025).
14. S. Greenstein and M. Rosenbluh, "The influence of nonlinear spectral bandwidth on single longitudinal mode intra-cavity second harmonic generation," Opt. Commun. **248**(1-3), 241–248 (2005).
15. H. Lu, J. Su, Y. Zheng, *et al.*, "Physical conditions of single-longitudinal-mode operation for high-power all-solid-state lasers," Opt. Lett. **39**(5), 1117–1120 (2014).
16. W. Koechner, *Solid-State Laser Engineering* (Springer, 2006), Chap. 1.
17. K. I. Martin, W. A. Clarkson, and D. C. Hanna, "Self-suppression of axial mode hopping by intracavity second-harmonic generation," Opt. Lett. **22**(6), 375–377 (1997).